Noise Measurements on dc SQUIDs with Varied Designs*†

M.R. Condron II, G.M. Gutt, B. Muhlfelder, J.M. Lockhart#, J.P. Turneaure
Hansen Experimental Physics Laboratory, Stanford University, Stanford, CA 94305

M.E. Huber, M.W. Cromar, E.K. Houseman
National Institute of Standards and Technology, 325 Broadway, Boulder, CO 80303

* Supported by NASA under contract NAS8-36125

Also with Physics and Astronomy Dept., San Francisco State University

Abstract. We have fabricated and tested two types of SQUIDs. The first, a low inductance stripline device, was characterized using a commercial dc SQUID as a following amplifier. The second type was well coupled to a 0.16μH input coil and was characterized and flux-locked using an ultralow noise room temperature preamplifier. We present device characterization and noise data for both types of devices.

1. Introduction

An important application for SQUID magnetometers is the detection of very small signals from inductive receivers. In our application, the relativity gyroscope experiment [1], a dc SQUID must efficiently couple to a 1μH source inductance and must have low noise at a signal frequency of 1.6mHz. The well coupled, single transformer, washer type SQUIDs (WCS) we have studied here often display undesirable parasitic LC resonances in their characteristics. Several approaches aim to reduce the effects of these resonant structures through the use of damping [2,3,4,5]. A quantitative study of the effect of parasitic capacitance on dc SQUID performance was made by Ryhänen, *et al.* [6]. We investigated several damping configurations and found that the addition of a resistor between the SQUID's input coil and SQUID loop adequately controls the most significant resonances. SQUIDs often exhibit excess low frequency noise whose power spectral density scales as $f^{-\alpha}$ where α is commonly near unity. For the gyroscope experiment's 1.6mHz signal, the SQUID's $f^{-\alpha}$ noise far exceeds the white noise. To better understand the low frequency noise, we have studied both WCS devices of the design as described above and weakly coupled, stripline SQUID (SLS) devices, previously characterized by Huber and Cromar, with $f^{-\alpha}$ noise extending to relatively high frequencies [7].

2. Experimental Apparatus

The SLS test probe is shown in Fig. 1. Extensive electrostatic shielding was used as well as dual π-section filters on all leads. Ferromagnetic shielding reduced the dc magnetic field at the SLS to less than 0.5μT and superconductive enclosures provided ac magnetic shielding. An opto-isolated data acquisition system allowed automated collection of I-V and V-Φ characteristics. The SLS was operated in vacuum allowing a commercial ac conductance bridge/PID system to control temperature. We report data taken at 4.2K.

SLS noise is measured by coupling the device to a following commercial dc SQUID through a transformer-filter network which provides a low frequency current step-up of 4X.

Experiments on the WCS were made in similar probes at Stanford and at NIST (without the vacuum and temperature control feature). Flux locking was accomplished using an ultralow

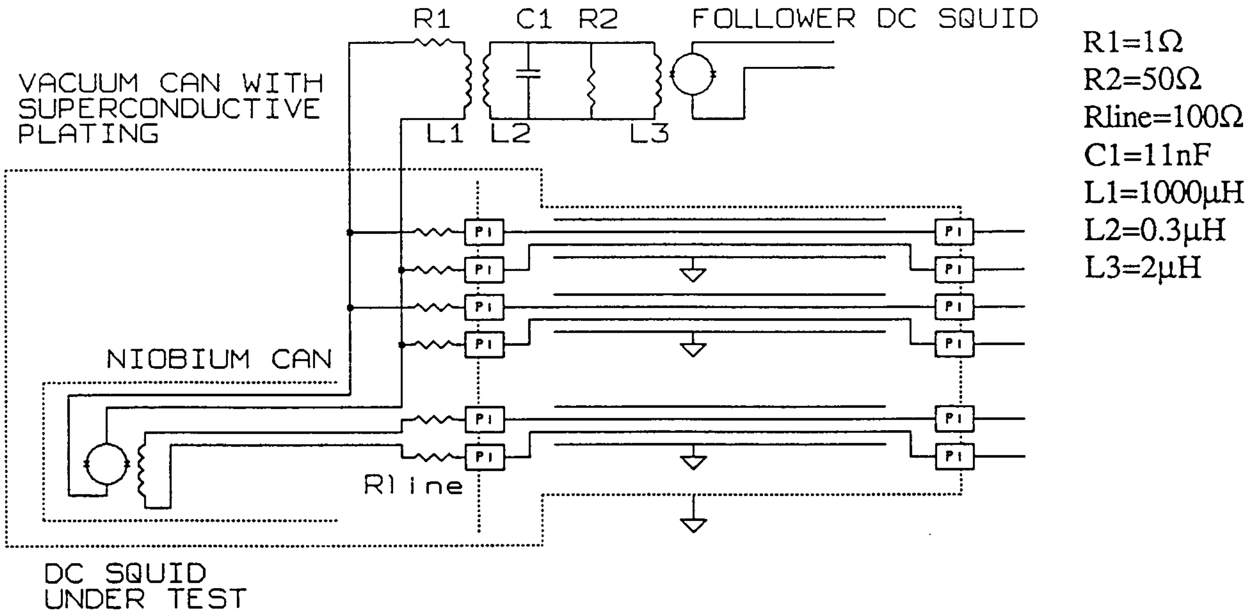

Figure 1: SLS test probe.

noise (0.33nV/$\sqrt{\text{Hz}}$) amplifier [8] with 100kHz modulation and two-pole integrator electronics similar to the design of Wellstood, *et al.* [9].

3. Device Fabrication

The SQUIDs were fabricated at NIST using a superconducting integrated circuit process with 2.5μm minimum feature size and based on Josephson junctions formed from Nb/Al-oxide-Al/Nb trilayers. The trilayers were formed on 51mm Si wafers whose temperature during deposition was maintained below 70°C. The load locked deposition system was cryopumped to its base pressure of 5.3 x 10^{-6}Pa and the lower Nb electrode (200nm thick) was sputtered in 1.07Pa of Ar at a rate of 2.5nm/s. Next, the Al layer (7nm thick) was sputtered in 0.67Pa of Ar at a rate of 0.1nm/s. The wafer was then transferred to the load-lock and the Al was oxidized in O_2 for 30 minutes to form the tunneling barrier. The wafer was returned to the deposition chamber and the upper Nb electrode (50nm thick) was sputtered in 1.07Pa of Ar at a rate of 1.5nm/s. The resulting trilayers were patterned by reactive ion etching in CF_4 and O_2. The junction shunting and resonance damping resistors are thermally evaporated $AuIn_2$ with sheet resistivity of approximately 1Ω/□. Insulating layers are thermally evaporated SiO and the SQUID washer and wiring layers are composed of thermally evaporated PbInAu alloy. All layers except the trilayer were patterned by photoresist lift-off.

4. Results

The I-V and V-Φ characteristics for the SLS were acquired with the following SQUID removed; the latter is shown in Fig. 2. The corresponding electrical parameters are given in Table 1. The junction shunt resistance, R_S, and the minimum and maximum critical currents (I_{CMIN} and I_{CMAX}) were inferred from the I-V curve. The SQUID's self inductance L_S was obtained from I_{CMIN} and I_{CMAX} using the work of Peterson and Hamilton [10]. The capacitance and the hysteresis

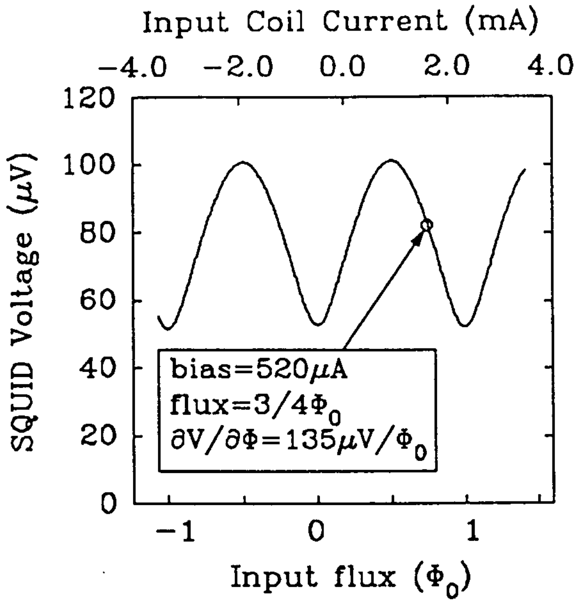

Figure 2: V-Φ curve for SLS.

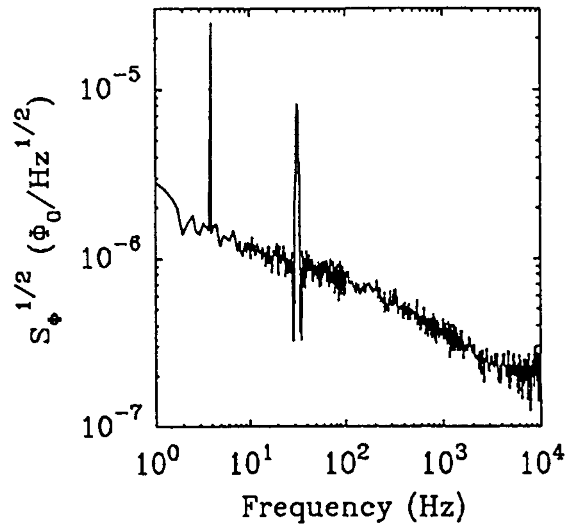

Figure 3: $\sqrt{S_\Phi}$ for SLS at state in Fig. 2.

parameter β_C were inferred from the area of the junction and its expected capacitance per unit area. The voltage noise spectral density was measured at the output of the following SQUID and normalized with the responsivity to yield $\sqrt{S_\Phi}$ (Fig 3). This verifies previous measurements taken from 1-1000Hz at NIST, however, the data shown here has slightly higher values of S_Φ. The difference may be due to helium boiling at 4.0K at NIST and 4.2K at Stanford. The origin of the spikes in Fig. 3 is not known.

The characteristics for the WCS without damping showed much more structure than for the SLS. The WCS V-Φ characteristics shown in Fig. 4 illustrate the improvement achieved when a damping resistor joins the input coil to the SQUID loop. The device parameters for a similar WCS are given in Table 1. The WCS coupling coefficient, k, was determined from a measurement of the mutual inductance between the SQUID and input coil, M_{SI}, assuming $k=M_{SI}/(nL_S)$.

For flux-locking measurements on the WCS, a 0.2μH superconductive inductor was placed across the SQUID input coil to simulate a typical source. The SQUID was biased at 43μA and the dc flux was adjusted to a minimum in the V-Φ characteristic. A 100kHz rounded square

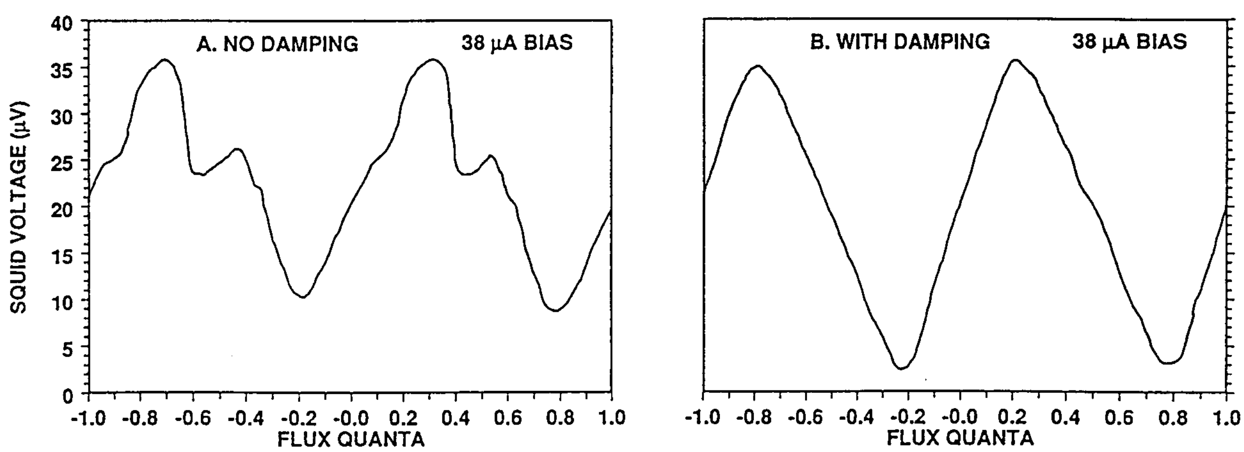

Figure 4: V-Φ curves for WCS without (A) and with damping (B).

	SLS	WCS
Critical Current ($2I_{CMIN}/2I_{CMAX}$)	220μA/440μA	30μA/45μA
$\beta_L=2L_SI_{CMAX}/\Phi_0$	0.95	1.8
$\beta_C=2\pi I_{CMAX}R_S^2C/\Phi_0$ (calculated)	0.3	0.05
L_S	4.5pH	83pH
L_I (calculated)	-	0.16μH
Washer to Input Resistance	Open	29.2Ω
R_S (junction shunt resistance)	0.66Ω	2.8Ω
M_{SI} (SQUID to input coil)	-	3.80nH
M_{SM} (SQUID to modulation coil)	0.73pH	49pH
k	-	0.96
n (input coil turns ratio)	-	44
Typical maximum responsivity	150μV/Φ_0	120μV/Φ_0

Table 1: dc SQUID Parameters

wave was then injected into the modulation coil. The measured white noise of the flux-locked SQUID (5μ$\Phi_0/\sqrt{Hz}$ between 50-2000Hz) was dominated by amplifier noise (no cold transformer used so far). The low frequency noise was 36μ$\Phi_0/\sqrt{f}$ for f between 1 and 20Hz.

5. Conclusion

The stripline SQUID exhibited smooth characteristics and a white noise level of $2 \times 10^{-7}\ \Phi_0/\sqrt{Hz}$. Below 4kHz the noise began to rise, yielding a power spectral density which scaled as approximately $f^{-0.5}$. The undamped WCS showed considerable structure in its I-V and V-Φ characteristics, presumably due to resonance effects. The addition of a damping resistor between the input coil and the SQUID loop appeared to control the dominant resonances, as evidenced by the smooth V-Φ curve. When flux-locked, the latter SQUID showed a white noise level dominated by electronics noise ($5 \times 10^{-6}\ \Phi_0/\sqrt{Hz}$) and low frequency noise which began to rise at about 20Hz with a $f^{-1.0}$ power spectral density. Further work is underway to determine the ultimate flux-locked noise performance of the damped WCS described here.

References:

1. J.M. Lockhart, Proc. SPIE **619**, 148 (1986).
2. K. Enpuku, K. Yoshida, and S. Kohjiro, J. Appl. Phys. **60**, 4218 (1986).
3. J. Knuutila, C. Ahonen, and C. Tesche, J. Low Temp. Phys. **68**, 269 (1987).
4. S. Kohjiro, K. Enpuku, K. Yoshida, and K. Yamafuji, Jpn. J. Appl. Phys. **27**, 1871 (1988).
5. V. Foglietti, W.J. Gallagher, M.B. Ketchen, A.W. Kleinsasser, R.H. Koch, and R.L. Sandstrom, Appl. Phys. Lett. **55**, 1451 (1989).
6. T. Ryhänen, R. Cantor, D. Drung, and H. Koch, IEEE Trans. Magn. **27**, 3013 (1991).
7. M.E. Huber and M.W. Cromar, Physica B **165&166**, 77-78 (1990).
8. G.M. Gutt, J.S. Kim, M.R. Condron II, J.M. Lockhart, and B. Muhlfelder, "An Ultralow Noise Amplifier for Superconductive Detectors." Submitted to *Superconductor Science and Technology*.
9. F. Wellstood, C. Heiden, and J. Clarke, Rev. Sci. Instrum. **55**, 952 (1984).
10. R.L. Peterson and C.A. Hamilton, J. Appl. Phys. **50**, 8135 (1979).